EWEA 2016 Annual Event - Abstract

Abstract title: CFD simulations of a wind turbine for analysis of tip vortex breakdown

Keita Kimura*, Yasutada Tanabe, Takashi Aoyama, Yuichi Matsuo, Chuichi Arakawa, Makoto Iida**

Keita Kimura, Chuichi Arakawa and Makoto Iida, The University of Tokyo, 7-3-1 Hongo, Bunkyo-ku, Tokyo, Japan
Yasutada Tanabe, Takashi Aoyama, Yuichi Matsuo, Japan Aerospace Exploration Agency, 7-44-1 Jindaijihigashimachi, Chofu-shi, Tokyo, Japan

Key Words: Wind Turbine, CFD, Wake, Tip vortex

1. Introduction

For economical use of wind turbines, it is important to install them collectively at one site (wind farm). Because of the collective layout of the wind turbines, we can reduce the total length of power transmission lines and labour for maintenance. However, the wake behind the wind turbines is known to cause major problems when the turbines are in a collective layout. A wind turbine converts the kinetic energy of wind into mechanical energy; consequently, the speed of the wind in the wake region is greatly reduced. Moreover, the existence of tip vortices impedes momentum exchange between the wake and the main stream[1]. In other words, velocity deficits of the wind turbine wake tend to remain at a long distance because of the tip vortices. In addition, when these vortices directly flow in a subsequent wind turbine, its fatigue gets accumulated faster. For the above reasons, each wind turbine in a wind farm is placed away from the others. Practically, a distance of 10D (D is the diameter of the wind turbines) between two rotors is recommended[2]. However, this criterion is determined empirically, and the optimum distance is supposed to vary depending on the operational conditions. Therefore, we must investigate the wake structure using scientific approaches for the optimum layout of the wind farms.

In general, experimental approaches or numerical studies are considered to study the wake structure. The experimental approaches' results typically tend to be reliable because we can consider the actual phenomena. However, performing an experiment on wind turbines is increasingly difficult because the size of the commercial wind turbines is increasing. At present, the rotor diameters of the commercial wind turbines are approximately 100 m and will increase to approximately 200 m in the future, making it very expensive to perform experiments. Alternatively, numerical studies do not require such construction costs. In addition, the entire field data can be obtained via computational fluid dynamics (CFD). At present, we can predict the average flow fields around the wind turbines using CFD[3]. However, discussion on the behaviour of the tip vortices is ongoing. Understanding the wake structure is a difficult subject to study and we aim to achieve it.

In this study, we conducted the CFD simulation of the wind turbines to study the vortex structure and the breakdown process by using a higher order scheme and dynamic calculations. We changed the tip speed ratio λ (TSR) to investigate the relation between TSR and the tip vortex structures.

*Presenting author. ** Corresponding author.
E-mail: k.kimura@gg.cfdl.t.u-tokyo.ac.jp (Keita Kimura),
iida@ilab.eco.rcast.u-tokyo.ac.jp (Makoto Iida)

2. Approach

2-1. Analysis objective

We selected the model wind turbine which was used in Model Experiments in Controlled Conditions (MEXICO) project as our study topic[4][5][6]. One of the special features of the test is that it includes the particle image velocimetry measurement of the near wake region. Therefore, such data can be used to validate the CFD results of the distributions of velocity and/or vorticity. The specifications for MEXICO are shown in Table 1.

Table 1. Specifications of MEXICO experiments

Rotor diameter [m]	4.5		
Blade length [m]	2.05		
Number of blade [-]	3		
Speed of main flow[m/s]	10	15	24
Tip speed ratio [-]	10	6.67	4.17
Rated number of revolution [rpm]	424.5		
chord length [m]	0.113 (at 0.82% span)		
Reynolds number	8×10^5		

2-2. Analysis code

In this study, we used the Moving Overlapped Structured Grids CFD Solver rFlow3D[7], which was developed by the Japanese Aerospace eXploration Agency (JAXA) for analysing rotorcrafts such as helicopters. The governing equations are the compressible Navier–Stokes equations, which are discretised using a finite volume method (FVM). rFlow3D can address moving overlapped grids; thus, it can simulate the blade rotations and deformations.

2-3. Computational grid

We set two background Cartesian grids and three rotating blade grids for analysis. Furthermore, we established an inner background grid, which has high grid resolution to capture the small structure of the tip vortices. The grid covers from 0.5 rotor diameters upwind of the rotor plane to 10 rotor diameters downwind. Details of the computational grids are presented in Table 2 and Figs. 1 and 2.

Table 2. Computational grid information.

	Blade Grid	Inner Background Grid	Outer Background Grid
Number of partition (I×J×K)	121 × 121 × 61	1311 × 187 × 187	151 × 101 × 101
Computational domain (D = 4.5m)	-	$10.5D \times 1.3D \times 1.3D$	$14.5D \times 5D \times 5D$
Minimum space [m]	1.0e-5 ($y^+ \approx 1$)	0.036	0.036
Total number of cells	48 millions		

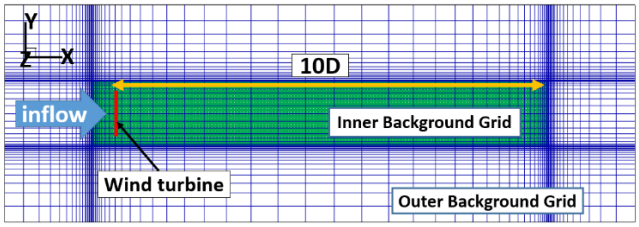

Fig. 1. Computational grid around the wake region

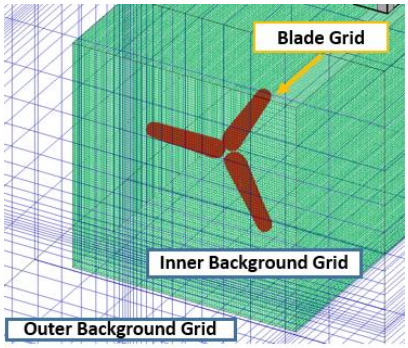

Fig. 2. Setup of the Computational grids

2-4. Numerical analysis condition

In this study, we performed an unsteady Reynolds-averaged Navier–Stokes simulation of the wind turbines. The numerical analysis conditions are shown in Table 3. We used a fourth-order compact MUSCL TVD [7] interpolation scheme as the reconstruction method. Thus, the resolution in space is fourth-order, enabling us to precisely capture even small vortices. The operational conditions are the same as those in Table 1.

Table 3. Numerical analysis condition.

Governing equations	Reynolds-averaged Navier-Stokes equations
Space discretization	Cell-vertex FVM (Background) Cell-centered FVM (Blade Grid)
Inviscid flux	SLAU[8]
Reconstruction	4th order Compact MUSCL TVD interpolation[7]
Turbulence model	Spalart-Allmaras[9]
Rotation of wind turbine	Moving Overlapped Structured Grids
Time integration	4th order Runge-Kutta (Background) LU-SGS/LU-DUR implicit method (Blade Grid)

3. Main body of abstract

3-1. Validation of CFD results

First, we must validate our results by comparing them with the results of the MEXICO experiments. We executed a case, $\lambda = 6.67$, which is the standard condition for operating the wind turbines. The axial velocity along the spanwise position $r = 1.8$ at azimuth angle of 270° is shown in Fig. 3. Although the CFD result slightly underpredicts the velocity deficit around the rotor position ($x/D = 0$), it shows good agreement with MEXICO in the wake region. The positions of the vortex core are shown in Fig. 4. rFlow3D is found to reproduce the wake expansion of MEXICO well.

From these two points of view (velocity deficit and wake expansion), we consider that our simulation captured at least the macro characteristics of the wind turbine wake.

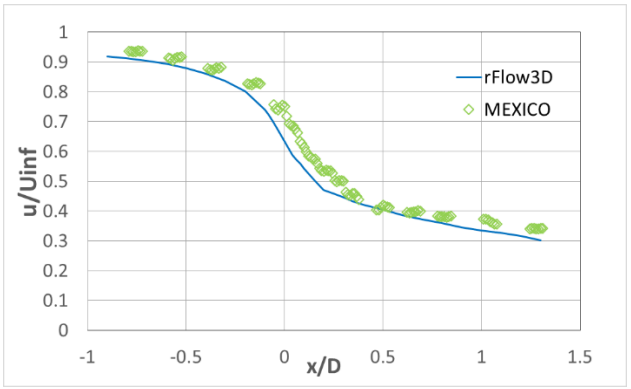

Fig. 3 . Axial traverse of axial velocity ($\lambda = 6.67$)

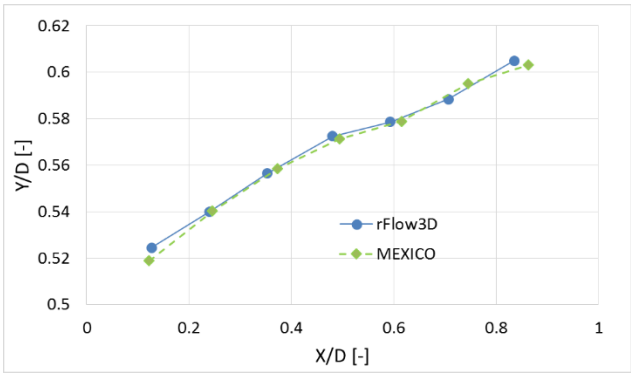

Fig. 4. Positions of tip vortex core. ($\lambda = 6.67$)

3-2. Wake expansion and breakdown of tip vortex

Further, we executed the other case by changing TSR to focus on the relation between the behaviour of vortices and TSR. Similar to section 3-1, we obtained the positions of the tip vortex core as shown in Fig. 5. When TSR increases, the wake expansion rate also increases. This behaviour is supposedly caused by changing the ratio of the centrifugal force and the main stream velocity. Moreover, the wake expansion rate should involve the starting position of the vortex instability. The iso-surface of vorticity is shown in Fig. 6. At the initial stage of wake, the tip vortices are stable and do not have any minute structure. Subsequently, the vortices begin to interact with each other and short wavelength instabilities appear. Finally, the helical structures completely break down. When TSR increases, the space between each vortex reduces. Consequently, the interaction

of the vortices increases. In the case of $\lambda = 4.17$, the wake disturbance begins at $x \cong 2D$, for $\lambda = 6.67$, it begins at $x \cong 1D$ and for $\lambda = 10$, it can be observed at $x \cong 0.5D$.

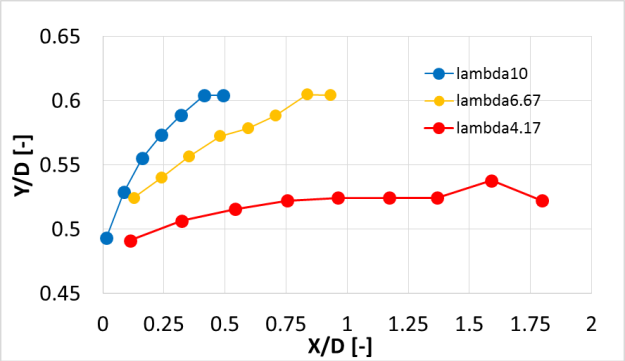

Fig. 5. Positions of tip vortex core
(red: $\lambda = 4.17$, yellow: $\lambda = 6.67$, blue: $\lambda = 10$)

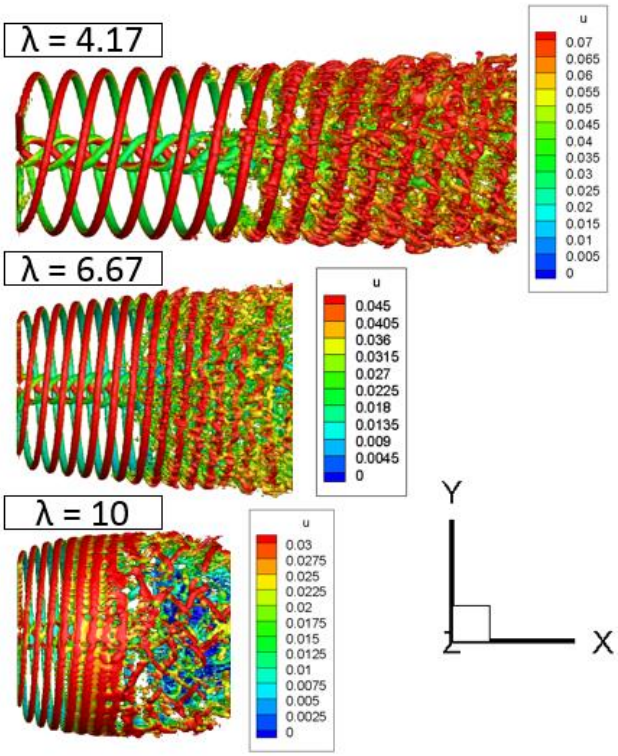

Fig. 6. Iso-surfaces of vorticity = 0.2 [/s]
colored by the streamwise velocity
(Top : $\lambda = 4.17$, Meddle : $\lambda = 6.67$, Bottom : $\lambda = 10$
Vorticity and velocity are scaled by speed of sound)

3-3. Radial flows in wake region

In this section, we focus on the distribution of radial flow behind the rotor plane. Radial flows must correspond to radial expansion of the tip vortices shown in Fig. 5. To visualise radial flows, we converted the Cartesian velocities (v, w) into cylindrical velocities, as shown in Fig. 7; subsequently, the radial velocity V_r (1) and azimuthal velocity V_ψ (2) are derived.

$$V_r = v \sin\psi + w \cos\psi \quad (1)$$

$$V_\psi = v \cos\psi - w \sin\psi \quad (2)$$

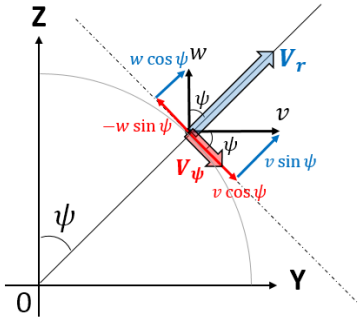

Fig. 7. Decomposition velocities of Cartesian coordinate system into radial and azimuthal velocities

The distribution of V_r is shown in Fig. 8. The left column shows the plane at $x = 0.25D$ as an example of the stable region of the tip vortices. Each TSR case has a yellow circular area, i.e., a relatively strong radial flow towards the outside of the plane. Because of these radial velocities, wake expansion occurs. Note that the strong red and blue regions represent the cross-sections of the tip vortices. The right column shows the planes at the region of vortex instabilities for each TSR. Because of the occurrence of the tip vortex breakdown, small vortices are diffused into the entire surface, leading to disappearance of the radial flow. Alternatively, the wake expansion stops and the tip vortex becomes unstable. As mentioned in the previous section, when TSR increases, the tip vortex breakdown starts earlier. However, note that V_r strengthens at the same time. The existence of V_r can act as a barrier that prevents the wake from mixing with the main stream because it is necessary for mixing to take the main stream into the wake. Therefore, a large value of TSR does not necessarily correspond to significant mixing of the wake.

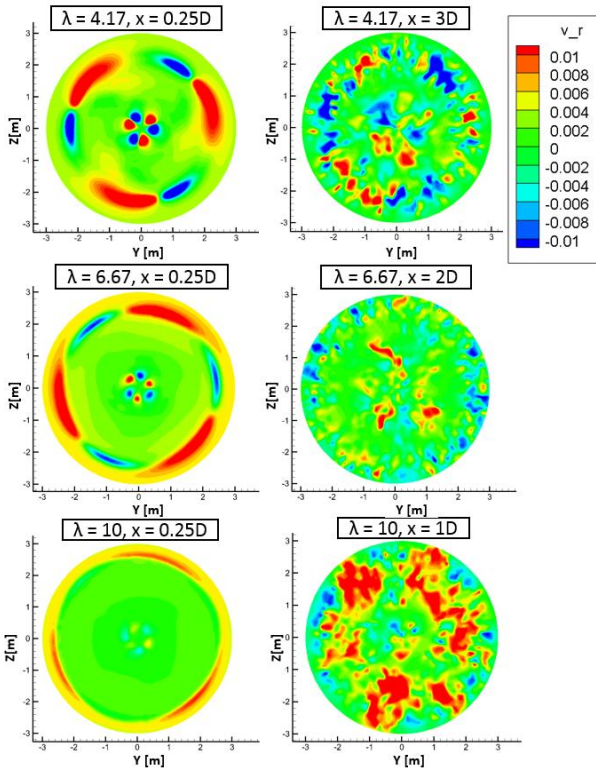

Fig. 8. Distribution of V_r in wake region
(left column : the plane at $x = 0.25D$, right column : the plane at $x = 3D, 2D, 1D$ for $\lambda = 4.17, 6.67, 10$. V_r is scaled by speed of sound)

4. Conclusion

We executed CFD simulations of the MEXICO rotor and implemented validations of the near-wake characteristics comparing the results of the MEXICO project. Furthermore, we considered two cases by changing TSR to investigate the relation between TSR and the wake structure. From these results, to date, we can conclude the following:

・The macro characteristics such as velocity distribution and vortex positions obtained by rFlow3D are generally consistent with the MEXICO experiments.

・When TSR increases, the radial wake expansion rate also increases.

・When TSR increases, the space between each vortex decreases. Therefore, the interaction between vortices increases and the tip vortex breakdown occurs more rapidly.

・During the beginning of vortex instabilities, wake expansion ceases because the radial flow produced by centrifugal forces disappears as a result of the breakdown of the tip vortices.

・Rapid breakdown of the tip vortices does not always correspond to rapid mixing of the wake with the main stream because this condition is often accompanied with a strong radial flow, which can be a barrier to wake mixing.

5. Learning objectives

In this study, we investigated the tip vortex breakdown by changing the tip speed ratio. Subsequently, we will attempt to evaluate the velocity deficits quantitatively by comparing with LiDAR measurements.

References

[1] Uchida, T. and Ohya. Y. and Sugitani, K. "Comparison between the wake behind wind turbine generator under op timal tip speed ratio and the wake behind stationary plate," *Proceedings of the 19th national symposium on wind engi neering*, p187-192, 2006.

[2] "The guidebook for Installation of wind power energy," NEDO, 2008. http://www.nedo.go.jp/content/100079735 (2016/04/13 accessed)

[3] L. Vermeer, J. Sørensen, and A. Crespo, "Wind tu rbine wake aerodynamics," *Progress in Aerospace Sci ences,* 2003-Vol.39, (2003), p467-510

[4] J.G. Schepers, K. Boorsma, *et al*. "Final report of IEA Wind Task 29: Mexnext (Phase 1)." ECN-E 12-004. 2012

[5] J.G. Schepers, K. Boorsma, *et al*. "Final report of IEA Wind Task 29: Mexnext (Phase 2)." ECN-E 14-060. 2014

[6] J.G.Schepers, H. Snel, *et al*. "Model Experiments in Controlled Conditions Final Report." ECN-E-07-042. 2008

[7] Tanabe, Y. and Saito, S., "Significance of all-speed scheme in application to rotorcraft cfd simulations," *The 3rd International Basic Research Conference on Rotorcraft Technology*. 2009

[8] Shima, E. and Kitamura, K., "On New Simple Low-Dissipation Scheme of AUSM-Family for All Speeds," *AIAA* 2009-136, 2009, pp.1-15.

[9] Spalart, P. R. and Allmaras, S. R., "A One-Equation Turbulence Model for Aerodynamic Flows," *AIAA*-92-0439, (1992)